JOURNAL OF CATALYSIS **172,** 370–379 (1997)
ARTICLE NO. CA971858

# Photocatalytic Reactions Involving Hydroxyl Radical Attack

## I. Reaction Kinetics Formulation with Explicit Photon Absorption Effects

Orlando M. Alfano, María I. Cabrera, and Alberto E. Cassano[1]

*Instituto de Desarollo Tecnológico para la Industria Química (INTEC), Universidad Nacional del Litoral (U.N.L.) and Consejo Nacional de Investigaciones Científicas y Técnicas (CONICET) Güemes 3450, (3000) Santa Fe, Argentina*

Received January 13, 1997; revised August 4, 1997; accepted August 5, 1997

**A kinetic model to represent the time evolution of a photocatalytic reaction is presented. It can be applied for reacting systems having the following characteristics: (i) the catalyst is a suspension (in water) of fine particles of titanium dioxide, (ii) the substrate is a hydrocarbon compound amenable to hydroxyl radical attack for the initiation of an oxidative reaction, (iii) the catalyst activation is produced by radiation energy in the near ultraviolet range (300 nm $\leq \lambda \leq$ 400 nm), (iv) oxygen is always present in the reacting medium, and (v) there are no mass transport limitations. The model is based on Turchi and Ollis (*J. Catal.* 122, 178 (1990)) proposed reaction sequence. The described formulation incorporates a precise and detailed evaluation of the radiation energy absorption effects. With this purpose the kinetic model is used in conjunction with a specially developed experimental device (Cabrera *et al.*, *Ind. Eng. Chem. Res.* 33, 3031 (1994); Alfano *et al.*, *Ind. Eng. Chem. Res.* 34, 488 (1995)) for which a one-dimensional–one-directional radiation and reactor model has been derived and validated. The model provides an explicit formulation for the radiation-absorbed effects that comprises in a single equation the cases of low and high irradiating conditions. The whole kinetic model development has been applied to the photodegradation of trichloroethylene in water, and it is the subject of a companion paper. Using this approach, reliable intrinsic kinetic data can be obtained.** 

### I. INTRODUCTION

The photocatalyzed degradation of organic environmental pollutants in the presence of a semiconductor catalyst has become a subject of increasing interest over the last 10 years since the pioneering work of Pruden and Ollis (4, 5) and Matthews (6, 7). In these investigations a redox reacting system is generated as a consequence of the formation of electrons and holes after the absorption of light of the appropriate wavelength by the semiconductor. Subsequent reaction of the generated pair with electron donors and acceptors leads to reactions that can produce the complete mineralization of water and air pollutants (8).

[1] To whom correspondence should be addressed. E-mail: ACASSANO@SILVA.ARCRIDE.EDU.AR.

The literature reports a variety of photocatalytic reactions involving several metal oxides (such as $TiO_2$, ZnO, $Fe_2O_3$, $WO_3$) as well as other semiconductors (CdS, for example) and a long list of organic and inorganic contaminants that in most cases can be fully decomposed (Matthews (9) and references therein). However, after due consideration to: (i) toxicity, (ii) photocorrosion resistance, (iii) availability, (iv) catalytic efficiency, and (v) cost, titanium dioxide stands alone in the preferred choice.

One of the most interesting processes based on titanium dioxide photocatalytic reactions in water systems is the mineralization reaction by which halogenated organic compounds can be converted into carbon dioxide, water, and halide ions. Removal of halogenated organic compounds is an important contribution to the solution of an environmental threat since most of these chemical substances exhibit rather high degrees of toxicity.

Several kinetic models for photocatalytic processes have been proposed (1, 10–13). There is general agreement that the main reaction path for the initiation of the degradation reaction of several hydrocarbon compounds appears to be an oxidative carbohydrogen bond cleavage by hydroxyl radical attack. Hydroxyl radicals are generated as a consequence of electron transfer to the semiconductor holes by adsorbed hydroxyl ions or water molecules (1).

Even if Turchi and Ollis' general proposal (1) could be different from the actual degradation detailed mechanism, it provides a sound approach based on a plausible "reaction scheme" that can be used to elaborate on rather simple kinetic models to describe the observed phenomena. As clearly stated by the authors "the chemical reaction steps occurring during photocatalysis are clearly numerous and complicated. The challenge to kineticists is to condense the system into a representation rate form of practical use."

In this work we have accepted the background information provided by Turchi and Ollis' contribution. We have developed an extension of their work based on their reaction sequence (steps 1–12; see Table 1), to render among other things, a more complete evaluation of radiation



0021-9517/97 $25.00

**TABLE 1**

**Reaction Scheme**[a]

| | | |
|---|---|---|
| Activation | $TiO_2 \xrightarrow{h\nu} e^- + h^+$ | [1] |
| Adsorption | $O_L^{2-} + Ti^{IV} + H_2O \leftrightarrow O_LH^- + Ti^{IV} - OH^-$ | [2a] |
| | $Ti^{IV} + H_2O \leftrightarrow Ti^{IV} - H_2O$ | [2b] |
| | $Site + R_i \leftrightarrow R_{i,ads}$ | [3] |
| | $OH\cdot + Ti^{IV} \leftrightarrow Ti^{IV} \mid OH\cdot$ | [4] |
| Recombination | $e^- + h^+ \rightarrow$ heat | [5] |
| Hole trapping | $Ti^{IV} - OH^- + h^+ \leftrightarrow Ti^{IV} \mid OH\cdot$ | [6a] |
| | $Ti^{IV} - H_2O + h^+ \leftrightarrow Ti^{IV} \mid OH\cdot + H^+$ | [6b] |
| | $R_{i,ads} + h^+ \leftrightarrow R_{i,ads}^+$ | [7] |
| Electron trapping | $Ti^{IV} + e^- \leftrightarrow Ti^{III}$ | [8a] |
| | $Ti^{III} + O_2 \leftrightarrow Ti^{IV} - O_2^-$ | [8b] |
| Hydroxyl attack | | |
| Case I | $Ti^{IV} \mid OH\cdot + R_{i,ads} \rightarrow Ti^{IV} + R_{j,ads}$ | [9] |
| Case II | $OH\cdot + R_{i,ads} \rightarrow R_{j,ads}$ | [10] |
| Case III | $Ti^{IV} \mid OH\cdot + R_i \rightarrow Ti^{IV} + R_j$ | [11] |
| Case IV | $OH\cdot + R_i \rightarrow R_j$ | [12] |

[a] Extracted from Turchi and Ollis (1).

absorption effects. In physical terms, the main differences of this approach with Turchi and Ollis' paper resides in the recognition that: (i) It does not seem necessary to decide beforehand which one of the four cases that are related to the actual adsorption states of the hydroxyl radicals and organic compounds prevails (which include the case of no adsorption and, consequently, reaction in the bulk of the liquid phase). A general expression considering the possibility of simultaneous occurrence of all of them can still render a minimum set of kinetic parameters to represent the reaction evolution. (ii) The required assumptions to obtain a simple kinetic expression have been reduced to a minimum; this minimum is in full agreement with a subset of those used in Turchi and Ollis' derivation. (iii) As should be expected in a practical system, due to the strong radiation extinction by the catalyst, both usually reported limiting cases for irradiation effects—low and medium to high levels of irradiation—may normally coexist in different regions of the same photoreactor. Then, a kinetic expression was obtained that will be applicable to the whole reactor regardless the irradiation level; this expression reproduces, as limiting cases, both dependencies—the linear and the square root functionality—with the local volumetric rate of radiation energy absorption (LVREA).

In a follow-up paper (14) all this development has been applied to the determination of the intrinsic kinetics of the decomposition of trichloroethylene in an oxygen-saturated solution using a suspended solid photocatalytic reactor for which the radiation field has been fully characterized (2, 3).

Three different but connected problems must be studied: (i) the reaction kinetics model, (ii) the development of the rate of electron-hole generation in a material particle of the solid suspension, and (iii) the model for characterizing the radiation field to evaluate the local volumetric rate of energy absorption (LVREA). With this approach, intrinsic and reliable kinetic information, i.e. independent of the reactor configuration and operating conditions, can be obtained.

## II. THE KINETIC MODEL

Let us consider Turchi and Ollis' proposal for the reaction sequence (1). It will be accepted as a plausible scheme for any system where hydroxyl attack on a C–H bond is the prevailing step for the oxidative breakdown of an organic contaminant, particularly for halogenated hydrocarbons. The required reaction path is illustrated in Table 1. The following components of the reaction sequence can be distinguished: (i) activation by radiation of the required wavelength to form the electron-hole pair, (ii) adsorption of water, the organic compound, and the hydroxyl radical on the surface of the catalyst (as a general approximation, none of them need to be always included or always disregarded), (iii) recombination of electron and holes (as the deactivation mechanism and one of the main causes for the low quantum efficiencies reported in these reactions), (iv) hole trapping by adsorbed species (furnishing reaction species for subsequent oxidation steps), (v) electron trapping, having oxygen as the main electron acceptor (this reaction is required to avoid photocorrosion of the catalyst), and (vi) hydroxyl attack (where all four possible cases have been included). Upon formation, the hydroxyl radical can: (a) interact with the solid by reverse reactions [6a] and [6b]; (b) react with the organic substance either in the adsorbed state or in a "free state" in the bulk of the fluid adjacent to the solid (reactions 9 and 11) and/or (c) migrate to the bulk of the adjacent fluid and react with adsorbed or "free" organic compound (reactions 10 and 12). (It will be shown that, to derive a simple working kinetic model there is no need to decide beforehand which one of the four possibilities correspond to the actual case.) Hole trapping is considered to be much more important in reactions involving adsorbed hydroxyl ions and/or water molecules; conversely, reaction [7], the direct trapping of holes by the organic substance has been reported as being less significant because of the lack of reactivity witnessed in water-free organic solutions. Electron trapping is supposed to occur through the participation of active sites of the solid (reaction 8a to form $Ti^{III}$) and further oxidation (reaction 8b) to form the superoxide ion. This is a brief summary of some of the main features of Turchi and Ollis' reaction scheme that will be used here. For more details, the interested reader is referred to the original work.

The effect of oxygen concentration has not been included in this proposal; hence, the kinetic model should be valid if and only if, oxygen concentration is not lacking in the fluid phase close to the catalytic particle. A second condition of applicability is the requirement of no mass transfer

limitations; this is a trivial statement that, notwithstanding, has been often neglected in many kinetic reports.

The following assumptions will be considered: (i) as indicated before, step 7 is not an important hole trapping reaction; (ii) whenever an adsorption process is surely involved in the sequence (reactions 3 and 4), it may be considered at equilibrium conditions; (iii) the steady state approximation may be applied for unstable reaction intermediates such as hydroxyl radicals and semiconductor holes; (iv) in dilute solutions of contaminants in water the concentrations of hydroxyl ions and water on the catalytic surface will be almost constant; (v) the catalytic surface (optical properties, specific surface area, and number of active sites) remains unchanged during the reaction; (vi) a rate of electrons and holes generation can be precisely defined; (vii) the recombination reaction of electrons and holes occurs mainly in the bulk of the catalytic particle; (viii) as a good approximation, the concentration of electrons and holes can be assumed equal; and (ix) the liquid phase does not absorb radiation in the near UV range (300 nm $\leq \lambda \leq$ 400 nm) and, consequently, there is no parallel homogeneous reaction. Assumptions (i), (ii), (iv), (vii), and (viii) have been discussed by Turchi and Ollis. Assumptions (iii) and (v) are fairly common in catalytic processes, particularly if catalyst poisoning is not considered; they were implicit or explicitly used in the above quoted reference. Assumption (vi) will be especially discussed in the next sections. Condition (ix) is generally satisfied by a large family of hydrocarbon compounds.

As indicated in Appendix A, with no further considerations, the following kinetic expression can be derived:

$$r_P = \frac{(k'_{6+}a_S)^2}{2k_5 v_P}\left\{-\left(\frac{E(R_i,R_j)}{1+E(R_i,R_j)}\right) + \sqrt{\left(\frac{E(R_i,R_j)}{1+E(R_i,R_j)}\right)^2 + \frac{4k_5 v_P}{(k'_{6+}a_S)^2}r_g}\right\} \times \frac{\alpha_{3,i}[R_i]}{(1+E(R_i,R_j))}. \quad [1]$$

In Eq. [1] $r_P$ is a reaction rate per catalytic particle. This equation can be rewritten as

$$r_P = \alpha'_1\left\{-\left(\frac{E(R_i,R_j)}{1+E(R_i,R_j)}\right) + \sqrt{\left(\frac{E(R_i,R_j)}{1+E(R_i,R_j)}\right)^2 + \frac{2}{\alpha'_1}r_g}\right\}\frac{\alpha_{3,i}[R_i]}{(1+E(R_i,R_j))}, \quad [2]$$

where

$$\alpha'_1 = \frac{(k'_{6+}a_S)^2}{2k_5 v_P}, \quad E(R_i,R_j) = \alpha_{3,i}[R_i] + \sum_{\substack{j=1\\(j\neq i)}}^{n}\alpha_{3,j}[R_j]. \quad [3]$$

Notice that: (i) excluding the evaluation of the rate of electron-hole generation ($r_g$), Eq. [2] has only two constants, $\alpha'_1$ and $\alpha_{3,i}$, and (ii) $\alpha_{3,i}$ is not an adsorption equilibrium constant (see Appendix A).

To apply Eq. [2] we must know the rate of electron-hole generation ($r_g$). It can be obtained from a radiation balance performed over the catalytic particles contained in a small volume of suspension.

## III. THE RATE OF ELECTRON-HOLE GENERATION ($r_g$)

In Eq. [2] we must obtain the value of the reaction rate for the initiation step (reaction 1 in Table 1).Consider now a small volume $V$; this volume is a portion of the heterogeneous system made of the liquid (L) and the particles of the solid catalyst (S). The volume $V$ is the sum of $V_L$ and $V_S$ ($V_S = \Sigma v_P$, is the solid volume existing in $V$). We will look for an expression of $r_g$ valid for any material point in the reacting space, i.e. a local value that is applicable to the suspension of the solid in the liquid phase ($r_g$ [=] mol s$^{-1}$ particle$^{-1}$). This is a requirement of the reaction kinetic formulation (see Eq. [A.10] in Appendix A). The following assumptions are needed: (i) radiation absorption is a bulk phenomenon that occurs through the irradiated surface of the catalyst; (ii) radiation absorption in a volume element is produced by all the semiconductor particles contained in that element; and (iii) upon radiation absorption, electrons and holes are generated with a primary quantum yield equal to $\phi_\lambda$. As is shown in Appendix B,

$$r_g(\mathbf{x},t) = \frac{1}{N_V}\int_{\lambda_1}^{\lambda_2} d\lambda\, \phi_\lambda e^a_\lambda(\mathbf{x},t). \quad [4]$$

In Eq. [4] the monochromatic LVREA [$e^a_\lambda(\mathbf{x}, t)$] is the result of the average absorption rate calculated over all the catalytic surface (area $A_S$ corresponding to $V_S$) existing in the volume $V$. The LVREA must be obtained from the solution of the radiative transfer equation (RTE) applied to each particular reactor.

## IV. EVALUATION OF THE LVREA

Despite the known difficulties that one encounters when dealing with a heterogeneous photocatalytic reactor (due to the existence of scattering), a reactor has been developed to perform kinetic studies in suspended solid systems. Alfano *et al.* (3) proposed a one-dimensional–one-directional model (1-Dim.–1-Dir. Model) for a rather simple experimental reactor. Figure 1 shows a schematic representation of the reactor. From the radiation point of view, the reactor design requires: (i) the window for radiation entrance must provide diffuse and uniform irradiation inside the reactor volume; this is accomplished by illuminating the plate of the reactor window with an almost uniform radiation flux and making the interior side of the plate

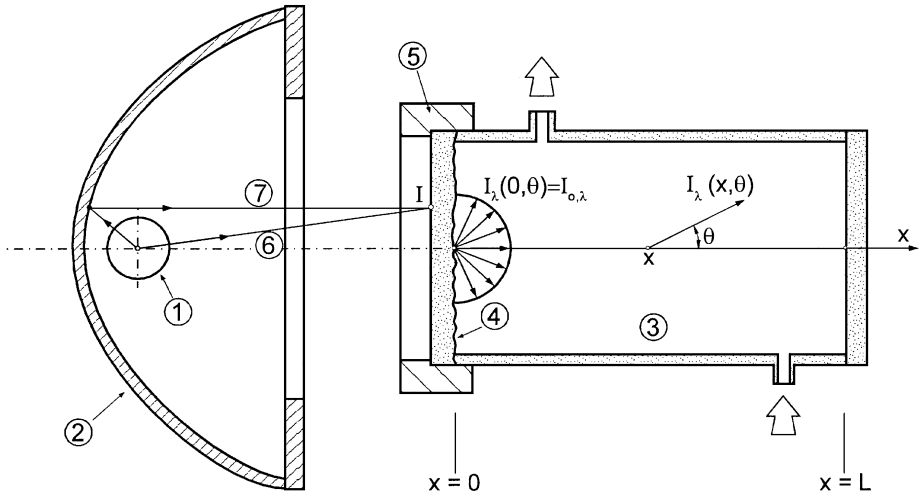


**FIG. 1.** Schematic representation of the photocatalytic reactor: ① lamp; ② parabolic reflector; ③ reactor; ④ reactor plate of radiation entrance; ⑤ nylon piece; ⑥ direct ray; ⑦ reflected ray.

of ground glass; (ii) radiation extinction inside the reactor must be high; this is controlled by the reactor length and the catalyst concentration. Under these conditions, the participating (absorption and scattering) and reacting (photocatalytic) medium can be rigorously represented by a mathematical model that uses a single spatial dimension (in a Cartesian coordinate system); also, since the reactor will have azimuthal symmetry (due to the imposed irradiating conditions), just one directional variable for radiation intensities will suffice (one angular coordinate in a spherical coordinate system).

The RTE for the 1-Dim.–1-Dir. Model is given by (15)

$$\mu\frac{\partial I_\lambda(x,\mu)}{\partial x}+\beta_\lambda I_\lambda(x,\mu) = \frac{\sigma_\lambda}{2}\int_{\mu'=-1}^{1} I_\lambda(x,\mu')p(\mu,\mu')\,d\mu' \qquad [5]$$

$$I_\lambda(0,\mu) = I_{0,\lambda}, \quad \mu > 0 \qquad [6]$$

$$I_\lambda(L,\mu) = 0, \quad \mu < 0. \qquad [7]$$

In Eq. [5], $\beta_\lambda$ and $\sigma_\lambda$ are the spectral, volumetric extinction and scattering coefficients, respectively. They can be obtained following special experimental procedures developed by Cabrera *et al.* (16). These authors have used a combination of conventional spectrophotometric measurements and special experiments that placed an integrating sphere at the outlet of the spectrophotometer sample cell. The almost conventional measurement gave the extinction coefficient (provisions were taken to minimize the scattering-in and maximize the scattering-out). The second type of detection collected all the nonabsorbed photons that are scattered in the forward direction. With a good degree of approximation, the results of the measurements with the integrating sphere provided a value that can be associated with that energy corresponding to forward scattering. The most simple radiative transfer model was applied to the spectrophotometer cell; thus, for each wavelength, the energy measured by the integrating sphere detector could be predicted using just a single adjustable parameter: the absorption coefficient (because the extinction coefficient was known from an independent determination). Using a nonlinear least square fitting, handled by an optimization program, this adjustment was made employing the model output and the experimental results. This method provides the volumetric absorption coefficient ($\kappa_\lambda$).

The phase function ($p$) is readily accessible for titanium oxide particle sizes or agglomerates larger than approximately 250 nm (for particle suspensions in water, and wavelengths between 300 and 400 nm); in this case, since the size parameter ($x = \pi n_\lambda d_P/\lambda$) is greater than 5, geometric optics applies. Considering the characteristics of the titanium oxide water suspensions, a diffuse reflectance phase function model, taken from the geometric optics (17), was assumed:

$$p(\mu_o) = \frac{8}{3\pi}\left(\sqrt{1-\mu_o^2} - \mu_o \cos^{-1}\mu_o\right). \qquad [8]$$

This assumption is known to be a limiting situation, but it should be a good approximation for clusters of titania of rather irregular shape, made by agglomeration of many small particles. It does not seem convenient to use other models (for example, the specular, partial reflection model) or the Mie theory. It is difficult to conceive some sort of specular reflection in the titanium oxide particles and, on the other hand, Mie theory strictly applies only to smooth, spherical particles. Besides, both approaches can be applied only if the complex refraction index as a function of wavelength is available; these values, to the best of our knowledge, are known only for the rutile variety of the semiconductor. Conversely, in order to apply the diffuse reflection phase function model the only significant assumption has

been to consider that the surface is an ideal diffuser (reflection is 100% diffuse).

Provided that $I_\lambda(0, \mu)$, $p(\mu, \mu')$, $\kappa_\lambda$, and $\sigma_\lambda$ are known, Eq. [5] can be solved. For usual catalytic systems, we must resort to approximate solutions or numerical techniques. Among the latter, it is recognized that the most accurate results are obtained with the discrete ordinate method (DOM) (18); besides, it is a very powerful tool for tackling a great variety of problems with almost no restrictions. The DOM transforms the integrodifferential equation (Eq. [5]) into a system of algebraic equations that can be solved by machine computation.

These equations are valid for monochromatic and coherent radiation in a system with absorption and multiple, anisotropic, and independent scattering (15). This type of scattering is typical of photocatalytic systems. Extension to polychromatic radiation can be done with the usual procedures (19). Its solution provides the radiation intensity field $[I_\lambda(x, \mu)]$ inside the reactor. Once this field is known, the LVREA at any point inside the reactor is immediately computed:

$$e^a_\lambda(x) = 2\pi\kappa_\lambda \int_{\mu=-1}^{1} I_\lambda(x, \mu)\, d\mu. \qquad [9]$$

The boundary condition at $x = 0$ (Eq. [6]), must be known beforehand. It is the result of irradiating the plate of the reactor window with a tubular lamp and a parabolic reflector. Thus, it can be obtained if the spectral radiative flux at the window of radiation entrance and the transmission coefficient of the window plate are known:

$$I_{0,\lambda} = \frac{1}{\pi} Y_{\mathrm{Pl},\lambda} \langle q_{T,\lambda}(r_I, \beta_I)\rangle_{A_{\mathrm{Pl}}}. \qquad [10]$$

The spectral transmission coefficient ($Y_{\mathrm{PI},\lambda}$) must be obtained for a wet plate made of ground glass and can be measured with a spectrophotometer (3). The area-averaged radiation flux can be obtained with an emission model for the tubular lamp-parabolic reflector irradiating system (20, 21). This model considers that every point on the irradiated surface (the reactor window plate) receives two types of contributions: (i) direct radiation from the lamp and (ii) reflected radiation from the reflector. Both can be predicted from the lamp, reactor, and reflector dimensions and characteristics (22). The area-average of direct and reflected radiation is obtained according to

$$\langle q_{T,\lambda}(r_I, \beta_I)\rangle_{A_{\mathrm{Pl}}} = \left(\frac{4}{\pi r^2_{\mathrm{Pl}}}\right) \int_0^{r_{\mathrm{Pl}}} r_I\, dr_I \int_0^{\pi/2} (q_{D,\lambda}(r_I, \beta_I) + q_{Rf,\lambda}(r_I, \beta_I))\, d\beta. \qquad [11]$$

The second boundary condition (at $x = L$) simply states that due to the expected large value of the extinction coefficient, almost no radiation arrives at the rear plate of the reactor and, consequently, there is no reflection.

Solving Eq. [5] with boundary conditions [6] and [7], the specific intensity is obtained. With Eq. [9] the LVREA can be immediately calculated as a function of position and time. This value is necessary to calculate Eq. [4].

## V. KINETIC EQUATION

Inserting a monochromatic form of Eq. [4] into Eq. [2] we get an expression of the reaction rate per particle and monochromatic radiation as follows:

$$r_{\mathrm{P}} = \alpha'_1 \left\{ -\left(\frac{E(R_i, R_j)}{1 + E(R_i, R_j)}\right) + \sqrt{\left(\frac{E(R_i, R_j)}{1 + E(R_i, R_j)}\right)^2 + \frac{2}{\alpha'_1 N_V} \phi_\lambda e^a_\lambda(\mathbf{x}, t)} \right\} \times \left(\frac{\alpha_{3,i}[R_i]}{1 + E(R_i, R_j)}\right). \qquad [12]$$

Using polychromatic radiation, if one defines

$$\bar{\phi} = \frac{\int_\lambda \phi_\lambda e^a_\lambda\, d\lambda}{\int_\lambda e^a_\lambda\, d\lambda}, \qquad [13]$$

the reaction rate results:

$$r_{\mathrm{P}} = \alpha'_1 \left\{ -\left(\frac{E(R_i, R_j)}{1 + E(R_i, R_j)}\right) + \sqrt{\left(\frac{E(R_i, R_j)}{1 + E(R_i, R_j)}\right)^2 + \frac{\alpha'_2}{C_{\mathrm{mp}}} \int_\lambda e^a_\lambda(\mathbf{x}, t)\, d\lambda} \right\} \times \left(\frac{\alpha_{3,i}[R_i]}{1 + E(R_i, R_j)}\right). \qquad [14]$$

In Eq. [14] we have defined

$$\alpha'_2 = \frac{2\, v_{\mathrm{P}} \rho_{\mathrm{P}} \bar{\phi}}{\alpha'_1}, \quad N_V = \frac{C_{\mathrm{mp}}}{v_{\mathrm{P}} \rho_{\mathrm{P}}}. \qquad [15]$$

Equation [14] has three constants: $\alpha'_1$, $\alpha'_2$, and $\alpha_{3,i}$. With respect to Eq. [2] the additional constant comes from the evaluation of $r_{\mathrm{g}}$.

Rearranging Eq. [14], the rate will take the form

$$r_{\mathrm{P}} = \alpha'_1 \left\{ -1 + \sqrt{1 + \frac{\alpha'_2}{C_{\mathrm{mp}}} \int_\lambda e^a_\lambda(\mathbf{x}, t)\, d\lambda \Big/ \left(\frac{E(R_i, R_j)}{1 + E(R_i, R_j)}\right)^2} \right\} \times \frac{\alpha_{3,i}[R_i] E(R_i, R_j)}{(1 + E(R_i, R_j))^2}. \qquad [16]$$

From Eq. [16] the following cases can be readily obtained:

*Case* I.

$$\frac{\alpha_2'}{C_{\mathrm{mp}}}\int_\lambda e_\lambda^a(\mathbf{x},t)\,d\lambda \gg \left(\frac{E(R_i,R_j)}{1+E(R_i,R_j)}\right)^2$$

$$r_{\mathrm{P}} \cong k_{\mathrm{I}}\sqrt{\int_\lambda e_\lambda^a(\mathbf{x},t)\,d\lambda}\,\frac{\alpha_{3,i}[R_i]}{1+E(R_i,R_j)}. \quad [17]$$

Equation [17] shows the typical square root dependence with respect to the LVREA and the Langmuir–Hinshelwood type dependence with respect to substrate concentrations.

*Subcase* I.a. $E(R_i, R_j) < 0.01$,

$$r_{\mathrm{P}} \cong k_{\mathrm{I}}\sqrt{\int_\lambda e_\lambda^a(\mathbf{x},t)\,d\lambda}\;\alpha_{3,i}[R_i]. \quad [18]$$

The reaction rate will have always a linear dependence with respect to the substrate concentration and will always show a square root dependence with respect to the LVREA.

*Subcase* I.b. $E(R_i, R_j) > 100$. The rate will take the form

$$r_{\mathrm{P}} \cong k_{\mathrm{I}}\sqrt{\int_\lambda e_\lambda^a(\mathbf{x},t)\,d\lambda}\,\frac{\alpha_{3,i}[R_i]}{E(R_i,R_j)}. \quad [19]$$

If only component $i$ is considered, i.e. $[R_j]=0$,

$$r_{\mathrm{P}} \cong k_{\mathrm{I}}\sqrt{\int_\lambda e_\lambda^a(\mathbf{x},t)\,d\lambda}. \quad [20]$$

The reaction rate will be independent of the substrate concentration and will show a square-root dependence with the LVREA.

*Case* II.

$$\frac{\alpha_2'}{C_{\mathrm{mp}}}\int_\lambda e_\lambda^a(\mathbf{x},t)\,d\lambda \ll \left(\frac{E(R_i,R_j)}{1+E(R_i,R_j)}\right)^2.$$

From a Taylor series expansion,

$$\sqrt{1+z} \cong 1+\tfrac{1}{2}z-\tfrac{1}{8}z^2+\tfrac{1}{16}z^3-\cdots \quad \text{valid for } (z^2<1) \quad [21]$$

$$\sqrt{1+z} \approx 1+\tfrac{1}{2}z \quad \text{valid for } z<0.5.$$

The rate will have the form

$$r_{\mathrm{P}} \cong k_{\mathrm{II}}\left(\int_\lambda e_\lambda^a(\mathbf{x},t)\,d\lambda\right)\frac{\alpha_{3,i}[R_i]}{E(R_i,R_j)}. \quad [22]$$

Equation [22] shows a linear dependence with the LVREA. Once more if only species $i$ is considered:

$$r_{\mathrm{P}} \cong k_{\mathrm{II}}\int_\lambda e_\lambda^a(\mathbf{x},t)\,d\lambda. \quad [23]$$

The reaction rate will be independent of the substrate concentration and will show a linear dependence with the LVREA.

## VI. CONCLUSIONS

A photocatalytic reaction kinetic-photocatalytic reactor model has been developed. It can be applied to decomposition reactions of hydrocarbons employing titanium dioxide suspended catalytic particles (Eq. [14]). The kinetic model is valid for a kinetic sequence where the oxidative path is initiated by hydroxyl radical attack on the C–H bond. It provides the decomposition rate of the substrate under a wide variety of operating conditions. The model does not account for changes in the oxygen concentration that has been assumed constant or in large excess.

The kinetics-reactor model permits the proper evaluation of the radiation energy absorption effects. It renders, as limiting cases, the usually reported linear and square root dependencies with the LVREA, depending on the reaction characteristics and operating conditions. However, in practical reactors both regimes will normally coexist as well as a "transition" operating condition. This means that in most cases the complete equation will have to be used.

The full reaction sequence can be well represented using only three reaction kinetic constants.

In a follow-up paper this models has been applied to the photocatalytic decomposition of trichloroethylene in water solution employing titanium dioxide as a catalyst.

## APPENDIX A: THE REACTION RATE PER PARTICLE

For a particle having a surface area equal to $a_{\mathrm{S}}$ and a volume equal to $v_{\mathrm{P}}$ the rate of disappearance of reactant $R_i$ is given by (see Table 1):

$$r_{\mathrm{P}} = k_9[\mathrm{Ti^{IV}\mid OH\cdot}][R_{i,\mathrm{ads}}]a_{\mathrm{S}}^2 + k_{10}[\mathrm{OH\cdot}][R_{i,\mathrm{ads}}]a_{\mathrm{S}} + k_{11}[\mathrm{Ti^{IV}\mid OH\cdot}][R_i]a_{\mathrm{S}} + k_{12}[\mathrm{OH\cdot}][R_i]. \quad [A.1]$$

Notice that $r_{\mathrm{P}}$ [=] mol of $R_i$ $\mathrm{s^{-1}}$ particle$^{-1}$, $k_9$ [=] particle $\mathrm{mol^{-1}\,s^{-1}}$, $k_{10}$ and $k_{11}$ [=] $\mathrm{m^3\,mol^{-1}\,s^{-1}}$, and $k_{12}$ [=] $\mathrm{m^6\,mol^{-1}\,s^{-1}}$ particle$^{-1}$. Concentrations in the bulk, such as [OH·] and $[R_i]$ must be thought of as those existing in the fluid film adjacent and very close to the catalytic particle.

The adsorbed organic substance concentration, $R_{i,\mathrm{ads}}$, and the concentration of the "association," $\mathrm{Ti^{IV}\mid OH\cdot}$, can be obtained assuming equilibrium for reactions 3 and 4. Then,

$$[R_{i,\mathrm{ads}}] = K_{3,i}[R_i][\mathrm{site}] \quad [A.2]$$

$$[\mathrm{Ti^{IV}\mid OH\cdot}] = K_4[\mathrm{OH\cdot}][\mathrm{Ti^{IV}}]. \quad [A.3]$$

Substituting Eqs. [A.2] and [A.3] into Eq. [A.1] we have

$$r_{\mathrm{P}} = \left\{k_9K_4[\mathrm{Ti^{IV}}]K_{3,i}[\mathrm{site}]a_{\mathrm{S}}^2 + k_{10}K_{3,i}[\mathrm{site}]a_{\mathrm{S}} + k_{11}K_4[\mathrm{Ti^{IV}}]a_{\mathrm{S}} + k_{12}\right\}[\mathrm{OH\cdot}][R_i]. \quad [A.4]$$

The steady state approximation can be applied to obtain the OH· concentration:

$$\begin{aligned} r_{\mathrm{OH}\cdot} = {} & k_{6+}[\mathrm{Ti^{IV}(OH)}][h^+]a_S - k_{6-}[\mathrm{Ti^{IV}} \mid \mathrm{OH}\cdot]a_S \\ & - k_9[\mathrm{Ti^{IV}} \mid \mathrm{OH}\cdot][R_{i,\mathrm{ads}}]a_S^2 - k_{10}[\mathrm{OH}\cdot][R_{i,\mathrm{ads}}]a_S \\ & - k_{11}[\mathrm{Ti^{IV}} \mid \mathrm{OH}\cdot][R_i]a_S - k_{12}[\mathrm{OH}\cdot][R_i] \\ & - \sum_{\substack{j=1 \\ (j\neq i)}}^{n} \big(k_{Rj,\mathrm{I}}[\mathrm{Ti^{IV}} \mid \mathrm{OH}\cdot][R_{j,\mathrm{ads}}]a_S^2 \\ & + k_{Rj,\mathrm{II}}[\mathrm{OH}\cdot][R_{j,\mathrm{ads}}]a_S + k_{Rj,\mathrm{III}}[\mathrm{Ti^{IV}} \mid \mathrm{OH}\cdot][R_j]a_S \\ & + k_{Rj,\mathrm{IV}}[\mathrm{OH}\cdot][R_j]\big) \cong 0. \end{aligned} \quad [A.5]$$

In Eq. [A.5] $[\mathrm{Ti^{IV}(OH)}]$ represents the superficial concentration of bound $OH^-$ or water. This is the species that it is assumed to react with the holes. In contaminated water systems Turchi and Ollis' assumption that this concentration may be fairly constant seems very acceptable. Hence,

$$k'_{6+} = k_{6+}[\mathrm{Ti^{IV}(OH)}]. \quad [A.6]$$

Substituting Eqs. [A.2], [A.3], and [A.6] into Eq. [A.5] one gets

$$\begin{aligned} [\mathrm{OH}\cdot] = \{k'_{6+}[h^+]a_S\} \Bigg/ \Bigg\{ & k_{6-}K_4[\mathrm{Ti^{IV}}]a_S \\ & + \big(k_9K_4[\mathrm{Ti^{IV}}]K_{3,i}[\mathrm{site}]a_S^2 \\ & + k_{10}K_{3,i}[\mathrm{site}]a_S + k_{11}K_4[\mathrm{Ti^{IV}}]a_S + k_{12}\big)[R_i] \\ & + \sum_{\substack{j=1 \\ (j\neq i)}}^{n} \big(k_{Rj,\mathrm{I}}K_4[\mathrm{Ti^{IV}}]K_{3,j}[\mathrm{site}]a_S^2 + k_{Rj,\mathrm{II}}K_{3,j}[\mathrm{site}]a_S \\ & + k_{Rj,\mathrm{III}}K_4[\mathrm{Ti^{IV}}]a_S + k_{Rj,\mathrm{IV}}\big)[R_j]\Bigg\}. \end{aligned} \quad [A.7]$$

If we call

$$\begin{aligned} \alpha_{3,i} = {} & \frac{k_9K_{3,i}[\mathrm{site}]a_S}{k_{6-}} + \frac{k_{10}K_{3,i}[\mathrm{site}]}{k_{6-}K_4[\mathrm{Ti^{IV}}]} + \frac{k_{11}}{k_{6-}} + \frac{k_{12}}{k_{6-}K_4[\mathrm{Ti^{IV}}]a_S} \\ \alpha_{3,j} = {} & \frac{k_{Rj,\mathrm{I}}K_{3,j}[\mathrm{site}]a_S}{k_{6-}} + \frac{k_{Rj,\mathrm{II}}K_{3,j}[\mathrm{site}]}{k_{6-}K_4[\mathrm{Ti^{IV}}]} + \frac{k_{Rj,\mathrm{III}}}{k_{6-}} \\ & + \frac{k_{Rj,\mathrm{IV}}}{k_{6-}K_4[\mathrm{Ti^{IV}}]a_S}. \end{aligned} \quad [A.8]$$

One gets

$$[\mathrm{OH}\cdot] = \frac{k'_{6+}}{k_{6-}K_4[\mathrm{Ti^{IV}}]} \times \frac{[h^+]}{1 + \alpha_{3,i}[R_i] + \sum_{\substack{j=1 \\ (j\neq i)}}^{n} \alpha_{3,j}[R_j]}. \quad [A.9]$$

Once more, the steady state approximation may be used to obtain the hole concentration:

$$r_{h^+} = r_g - k'_{6+}[h^+]a_S + k_{6-}[\mathrm{Ti^{IV}} \mid \mathrm{OH}\cdot]a_S - k_5[h^+][e^-]v_P \cong 0. \quad [A.10]$$

Here $r_g$ is the rate of electron-hole generation per particle ($r_g$ [=] mol $s^{-1}$ particle$^{-1}$). Following Turchi and Ollis (1), since photo-generation rates of electrons and holes are equal and the semiconductor intrinsic carrier density is comparatively low, we can also make the approximation that $[h^+] = [e^-]$. From Eq. [A.9] we can extract $[h^+]$ and substitute into Eq. [A.10]. From the resulting quadratic equation in $[\mathrm{OH}\cdot]$ one obtains:

$$\begin{aligned} [\mathrm{OH}\cdot] = {} & \frac{(k'_{6+})^2a_S}{2k_5v_Pk_{6-}K_4[\mathrm{Ti^{IV}}]} \Bigg\{ -\left(\frac{E(R_i, R_j)}{1 + E(R_i, R_j)}\right) \\ & + \sqrt{\left(\frac{E(R_i, R_j)}{1 + E(R_i, R_j)}\right)^2 + \frac{4k_5v_P}{(k'_{6+}a_S)^2}r_g}\Bigg\} \\ & \times \frac{1}{(1 + E(R_i, R_j))} \end{aligned} \quad [A.11]$$

In Eq. [A.11] we have defined

$$E(R_i, R_j) = \alpha_{3,i}[R_i] + \sum_{\substack{j=1 \\ (j\neq i)}}^{n} \alpha_{3,j}[R_j]. \quad [A.12]$$

Substituting Eqs. [A.8] and [A.11] into Eq. [A.4] and rearranging,

$$\begin{aligned} r_P = {} & \frac{(k'_{6+}a_S)^2}{2k_5v_P} \Bigg\{ -\left(\frac{E(R_i, R_j)}{1 + E(R_i, R_j)}\right) \\ & + \sqrt{\left(\frac{E(R_i, R_j)}{1 + E(R_i, R_j)}\right)^2 + \frac{4k_5v_P}{(k'_{6+}a_S)^2}r_g}\Bigg\} \\ & \times \frac{\alpha_{3,i}[R_i]}{(1 + E(R_i, R_j))}. \end{aligned} \quad [A.13]$$

This is equivalent to Eq. [1] of the paper.

## APPENDIX B : THE RATE OF ELECTRON-HOLE GENERATION

Consider a small volume ($V$) corresponding to the heterogeneous system. It is composed of the liquid (L) and many solid catalytic particles (S) and is located in a generic material point **x** with respect to a fixed coordinate system (Fig. B.1a). The position vector $\boldsymbol{\zeta}$ is referred to the local frame ($\zeta_1$, $\zeta_2$, $\zeta_3$) centered at **x**. This vector defines the position of any point inside the volume $V$. The solid catalytic particles are nonporous as is the case of many titanium dioxide varieties; typical examples are Aldrich Anatase and Degussa P 25$^{TM}$. Assume that the size of the solid particle

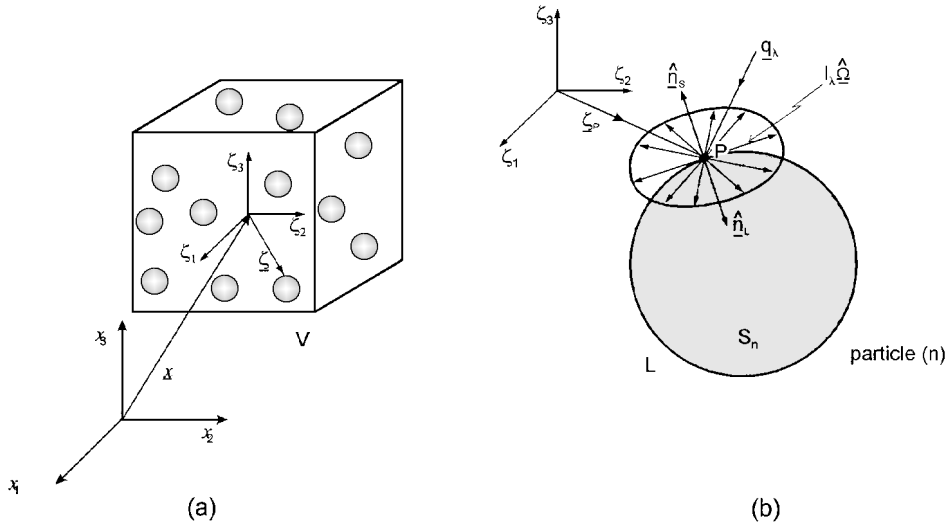


**FIG. B.1.** Absorption of radiation by a solid particle: (a) coordinate systems; (b) variables involved in the analysis of a single particle.

is larger than the working wavelength range, such as geometric optics are applicable.

Radiation absorption is a voluminal phenomenon that occurs after the impinging radiation crosses the bounding surface of the catalytic particle. Then, the photocatalytic activation is the result of a process that occurs by radiation impinging on the surface of the solid particle. Since the solid is nonporous, this process is initiated at the external surface of the particle. The orientation of this surface is characterized by its outwardly directed unit normal vector $\hat{\mathbf{n}}_S$ (Fig. B.1b). A point such as P on this surface collects different radiation intensities that may arrive from every direction in space included in the solid angle $4\pi$. Any radiation that after incidence on the surface moves backwards will be considered a "reflected" radiation (at this point it does not matter whether reflection is specular, diffuse, or has some other intermediate form). In this figure we have also represented the radiation flux vector defined at point P on the surface, for a given wavelength $\lambda$, resulting from the radiation field arriving at the surface point whose outward normal vector is $\hat{\mathbf{n}}_S$ : $[\mathbf{q}_\lambda = \int_{\Omega=4\pi} d\Omega I_\lambda \hat{\Omega}]$.

The rate of electron-hole generation at a point $P$ on the surface of particle "$n$," at a time $t$ and for a wavelength $\lambda$ (actually between $\lambda$ and $\lambda + d\lambda$) is

$$dr_{g,n,\lambda}(\mathbf{x}+\boldsymbol{\zeta}_P, t) = \phi_\lambda \left[ \int_{\Omega=4\pi} d\Omega I_\lambda(\mathbf{x}+\boldsymbol{\zeta}_P, t, \hat{\Omega})\hat{\Omega}\cdot\hat{\mathbf{n}}_L \right] dA$$
$$= \phi_\lambda [\mathbf{q}_\lambda(\mathbf{x}+\boldsymbol{\zeta}_P, t)\cdot\hat{\mathbf{n}}_L]\, dA, \qquad [B.1]$$

where $\phi_\lambda$ [=] mol einstein$^{-1}$ is an "activation step primary quantum yield" for the photocatalytic reaction.

Equation [B.1] can be integrated over the wavelength interval of the useful radiation range of interest (($\lambda_1$ and $\lambda_2$), accounting for the overlapping wavelength regions of lamp emission, reactor wall transmission (absorption and reflection), and radiation absorbing catalytic species absorption coefficient) and over the external area of the solid particle $A_{Sn}$:

$$r_{g,n}(\mathbf{x}, t) = \int_{\lambda_1}^{\lambda_2} d\lambda \phi_\lambda \int_{A_{Sn}} dA \left[ \int_{\Omega=4\pi} d\Omega I_\lambda(\mathbf{x}+\boldsymbol{\zeta}_P, t, \hat{\Omega})\hat{\Omega}\cdot\hat{\mathbf{n}}_L \right]$$
$$= \int_{\lambda_1}^{\lambda_2} d\lambda \phi_\lambda \int_{A_{Sn}} dA [\mathbf{q}_\lambda(\mathbf{x}+\boldsymbol{\zeta}_P, t)\cdot\hat{\mathbf{n}}_L]. \qquad [B.2]$$

According to Fig. B.1b, $\hat{\mathbf{n}}_L$ (the outwardly directed normal to the liquid phase) $= -\hat{\mathbf{n}}_S$ (the outwardly directed normal to the solid). Applying the divergence theorem to Eq. [B.2] we get

$$r_{g,n}(\mathbf{x}, t) = -\int_{\lambda_1}^{\lambda_2} d\lambda \phi_\lambda \int_{A_{Sn}} dA [\mathbf{q}_\lambda(\mathbf{x}+\boldsymbol{\zeta}_P, t)\cdot\hat{\mathbf{n}}_S]$$
$$= -\int_{\lambda_1}^{\lambda_2} d\lambda \phi_\lambda \int_{V_{Sn}} dV [\nabla\cdot\mathbf{q}_\lambda(\mathbf{x}+\boldsymbol{\zeta}_P, t)]. \qquad [B.3]$$

When there is no emission, it can be shown that a radiation balance for the radiation flux vector gives (15)

$$\nabla\cdot\int_{\Omega=4\pi} d\Omega\, I_\lambda\hat{\Omega} = \nabla\cdot\mathbf{q}_\lambda = -e^a_\lambda, \qquad [B.4]$$

where $e^a_\lambda$ is the local volumetric rate of energy absorption (the LVREA).

Substituting Eq. [B.4] into Eq. [B.3], the rate of electron-hole generation for particle "$n$" results:

$$r_{g,n}(\mathbf{x}, t) = \int_{\lambda_1}^{\lambda_2} d\lambda\, \phi_\lambda \int_{V_{Sn}} dV e^a_{\lambda,S}(\mathbf{x}+\boldsymbol{\zeta}, t). \qquad [B.5]$$

We must now relate the LVREA per particle, $e^a_{\lambda,S}(\mathbf{x}+\boldsymbol{\zeta}, t)$ to the LVREA by the suspension volume (liquid + solid), $e^a_\lambda(\mathbf{x}, t)$. The absorbed energy per unit wavelength interval,

unit time, and unit volume of the suspensions is

$$e^a_\lambda(\mathbf{x},t)=\frac{1}{V}\int_V dV e^a_\lambda(\mathbf{x}+\boldsymbol{\zeta},t). \qquad [B.6]$$

$V$ is the small suspension volume of the heterogeneous system located at point $\mathbf{x}$.

The right-hand side of Eq. [B.6] can be divided in two parts: (i) the radiation energy absorbed by the liquid and (ii) that part corresponding to the solid particles:

$$e^a_\lambda(\mathbf{x},t)=\frac{1}{V}\int_{V_\mathrm{L}} dV e^a_{\lambda,\mathrm{L}}(\mathbf{x}+\boldsymbol{\zeta},t)+\frac{1}{V}\int_{V_\mathrm{S}} dV e^a_{\lambda,\mathrm{S}}(\mathbf{x}+\boldsymbol{\zeta},t). \qquad [B.7]$$

In the small volume $V$ we have "$N$" solid photocatalytic particles; then, the right-hand side of Eq. [B.7] is

$$e^a_\lambda(\mathbf{x},t)=\frac{1}{V}\int_{V_\mathrm{L}} dV e^a_{\lambda,\mathrm{L}}(\mathbf{x}+\boldsymbol{\zeta},t)+\frac{1}{V}\left[\sum_{n=1}^{N}\int_{V_{\mathrm{Sn}}} dV e^a_{\lambda,\mathrm{S}}(\mathbf{x}+\boldsymbol{\zeta},t)\right]. \qquad [B.8]$$

Assuming that all particles are equal,

$$e^a_\lambda(\mathbf{x},t)=\frac{1}{V}\int_{V_\mathrm{L}} dV e^a_{\lambda,\mathrm{L}}(\mathbf{x}+\boldsymbol{\zeta},t)+\frac{N}{V}\int_{V_{\mathrm{Sn}}} dV e^a_{\lambda,\mathrm{S}}(\mathbf{x}+\boldsymbol{\zeta},t)$$
$$=\varepsilon_\mathrm{L}\left\langle e^a_{\lambda,\mathrm{L}}(\mathbf{x}+\boldsymbol{\zeta},t)\right\rangle_{V_\mathrm{L}}+N_V\int_{V_{\mathrm{Sn}}} dV e^a_{\lambda,\mathrm{S}}(\mathbf{x}+\boldsymbol{\zeta},t). \qquad [B.9]$$

In this equation $\varepsilon_\mathrm{L}$ is the liquid hold-up and $N_V=N/V$ is the number of particles per unit suspension volume.

Finally from Eqs. [B.5] and [B.9] we get

$$r_\mathrm{g}(\mathbf{x},t)=\frac{1}{N_V}\int_{\lambda_1}^{\lambda_2} d\lambda\,\phi_\lambda\left[e^a_\lambda(\mathbf{x},t)-\varepsilon_\mathrm{L}\left\langle e^a_{\lambda,\mathrm{L}}(\mathbf{x}+\boldsymbol{\zeta},t)\right\rangle_{V_\mathrm{L}}\right]. \qquad [B.10]$$

In our case the liquid does not absorb radiation in the wavelength range under consideration; then, the second term of the right-hand side (between brackets) is zero. However, if the liquid absorbs radiation, the complete Eq. [B.10] will be necessary to compute the rate of the heterogeneous activation step. When this is the case, that part of the radiation absorbed by the liquid must be incorporated into a separate initiation rate for the reaction mechanism in the homogeneous phase (with a homogeneous reaction quantum yield). On the other hand, to model the radiation field, radiation attenuation produced by absorption (in both phases) and scattering inside the system must be fully incorporated using an equation that accounts for the addition of the three concomitant processes.

Equation [B.10], simplified for the case in which the liquid is transparent, has been used in the paper as Eq. [4].

## APPENDIX C: NOTATION

| | |
|---|---|
| $A$ | area, $m^2$ |
| $a_\mathrm{S}$ | particle surface area, $m^2$ particle$^{-1}$ |
| $C_m$ | mass concentration, g $m^{-3}$ |
| $d_\mathrm{P}$ | nominal mean particle diameter, nm |
| $e^a$ | local volumetric rate of radiant energy absorption, einstein $m^{-3}$ $s^{-1}$ |
| $E(R_i, R_j)$ | parameter defined by Eq. [A.12] in Appendix A, dimensionless |
| $h^+$ | semiconductor valence band hole |
| $I$ | spectral radiation specific intensity, einstein $m^{-2}$ $sr^{-1}$ $s^{-1}$ |
| $k_i, k_i'$ | reaction rate constant (units depend of considered step) |
| $K$ | equilibrium adsorption constant, $m^3$ $mol^{-1}$ |
| $L$ | length, m |
| $n$ | refraction index, dimensionless |
| $\hat{\mathbf{n}}$ | unit normal vector, dimensionless |
| $N_V$ | number of particles per unit volume, particle $m^{-3}$ |
| $p$ | phase function, dimensionless |
| $q$ | radiative flux, einstein $m^{-2}$ $s^{-1}$ |
| $r$ | radius, m; also radial coordinate, m |
| $r_\mathrm{g}$ | rate of electron-hole generation, mol $s^{-1}$ particle$^{-1}$ |
| $r_\mathrm{P}$ | reaction rate per particle, mol $s^{-1}$ particle$^{-1}$ |
| $t$ | time, s |
| $v_\mathrm{P}$ | particle volume, $m^3$ particle$^{-1}$ |
| $V$ | volume, $m^3$ |
| $x$ | axial coordinate, m; also size parameter, dimensionless |

*Greek Letters*

| | |
|---|---|
| $\alpha_1'$ | kinetic parameter defined in Eq. [3], mol $s^{-1}$ particle$^{-1}$ |
| $\alpha_2'$ | kinetic parameter defined in Eq. [15], g s einstein$^{-1}$ |
| $\alpha_{3,i}, \alpha_{3,j}$ | parameters defined by Eq. [A.8] in Appendix A, $m^3$ $mol^{-1}$ |
| $\beta$ | volumetric extinction coefficient, $m^{-1}$; also cylindrical coordinate, rad |
| $\varepsilon$ | holdup, dimensionless |
| $\boldsymbol{\zeta}$ | position vector, m |
| $\theta$ | spherical coordinate, rad |
| $\kappa$ | volumetric absorption coefficient, $m^{-1}$ |
| $\lambda$ | wavelength, nm |
| $\mu$ | the quantity $\cos\theta$, dimensionless |
| $\rho$ | density, g $m^{-3}$ |
| $\sigma$ | volumetric scattering coefficient, $m^{-1}$ |
| $Y$ | transmission coefficient, dimensionless |
| $\phi$ | quantum yield, mol einstein$^{-1}$ |

$\bar{\phi}$ average value of $\phi$ over the wavelength interval, mol einstein$^{-1}$
$\hat{\mathbf{\Omega}}$ unit vector in the direction of radiation propagation, dimensionless

*Subscripts*

ads indicates adsorption
$A_{Pl}$ denotes plate area
$D$ denotes direct radiation
$i$ relative to species $i$
$I$ denotes an incident point
$j$ relative to species $j$
L denotes a liquid property
$n$ relative to particle $n$
P indicates a particle property
Pl denotes a plate property
Rf denotes reflected radiation
S denotes catalytic surface
$T$ denotes total value
$\lambda$ indicates a dependence on wavelength
$\mathbf{\Omega}$ indicates a dependence on direction of propagation
0 relative to the surface of radiation entrance
1 denotes a lower limit of integration
2 denotes an upper limit of integration
$+, -$ refer to the direct and reverse reaction, respectively

*Special Symbols*

$\langle\ \rangle$ indicates average value
$\vec{\ }$ denotes a vector quantity
[ ] denotes concentration

## ACKNOWLEDGMENTS

The authors are grateful to Consejo Nacional de Investigaciones Científicas y Técnicas (PID-201-1006) and to Universidad Nacional del Litoral (CAI+D-008-063 and 33-174) for their support to produce this work. Thanks are also given to Eng. Claudia Romani for technical assistance and Mrs. Silvana Wagner for helping in editing this manuscript.

## REFERENCES

1. Turchi, C. S., and Ollis, D. F., *J. Catal.* **122**, 178 (1990).
2. Cabrera, M. I., Alfano, O. M., and Cassano, A. E., *Ind. Eng. Chem. Res.* **33**, 3031 (1994).
3. Alfano, O. M., Negro, A. C., Cabrera, M. I., and Cassano, A. E., *Ind. Eng. Chem. Res.* **34**, 488 (1995).
4. Pruden, A. L., and Ollis, D. F., *Environ. Sci. Technol.* **17**, 628 (1983).
5. Pruden, A. L., and Ollis, D. F., *J. Catal.* **82**, 404 (1983).
6. Matthews, R. W., *J. Chem. Soc. Faraday Trans. 1* **80**, 457 (1984).
7. Matthews, R. W., *Water Res.* **20**, 569 (1986).
8. Ollis, D. F., Pelizzetti, E., and Serpone, N., *Environ. Sci. Technol.* **25**, 1523 (1991).
9. Matthews, R. W., *in* "Photocatalytic Purification and Treatment of Water and Air" (D. F. Ollis and H. Al-Ekabi, Eds.), p. 121. Elsevier Science, Amsterdam/New York, 1993.
10. Gerischer, H., *in* "Photocatalytic Purification and Treatment of Water and Air" (D. F. Ollis and H. Al-Ekabi, Eds.), p. 1. Elsevier Science, Amsterdam/New York, 1993.
11. Bahnemann, D., Bockelmann, D., Goslich, R., Hilgendorff, M., and Weichgrebe, D., *in* "Photocatalytic Purification and Treatment of Water and Air" (D. F. Ollis and H. Al-Ekabi, Eds.), p. 301. Elsevier Science, 1993.
12. Minero, C., *Sol. Energy Mater. Sol. Cells* **38**, 421 (1995).
13. Minero, C., Pelizzetti, E., Malato, S., and Blanco, J., *Solar Energy* **56**, 421 (1996).
14. Cabrera, M. I., Negro, A. C., Alfano, O. M., and Cassano, A. E., *J. Catal.* **172**, 380 (1997).
15. Ozisik, M. N., "Radiative Transfer and Interactions with Conduction and Convection," Wiley, New York, 1973.
16. Cabrera, M. I., Alfano, O. M., and Cassano, A. E., *J. Phys. Chem.* **100**, 20043 (1996).
17. Siegel, R., and Howell, J. R., "Thermal Radiation Heat Transfer," 3rd ed., Hemisphere, Bristol, PA, 1992.
18. Duderstadt, J. J., and Martin, R., "Transport Theory," Wiley, New York, 1979.
19. Clariá, M. A., Irazoqui, H. A., and Cassano, A. E., *AIChE J.* **34**, 366 (1988).
20. Alfano, O. M., Romero, R. L., and Cassano, A. E., *Chem. Eng. Sci.* **40**, 2119 (1985).
21. Alfano, O. M., Romero, R. L., and Cassano, A. E., *Chem. Eng. Sci.* **41**, 1155 (1986).
22. Cassano, A. E., Martín, C. A., Brandi, R. J., and Alfano, O. M., *Ind. Eng. Chem. Res.* **34**, 2155 (1995).